J Fail. Anal. and Preven. (2022) 22:690–703
https://doi.org/10.1007/s11668-022-01365-1

TECHNICAL ARTICLE—PEER-REVIEWED

A New Method for Rubbing Fault Identification Based on the Combination of Improved Particle Swarm Optimization with Self-Adaptive Stochastic Resonance

Haonan Cong · Mingyue Yu · Yunhong Gao · Minghe Fang

Submitted: 3 December 2021 / in revised form: 2 February 2022 / Accepted: 2 February 2022 / Published online: 22 February 2022

Abstract To fulfill the effective diagnosis of the rubbing fault between the rotor and the stator, the combination strategy of adaptive weight particle swarm optimization (PSO) and general scale transformation stochastic resonance (GSTSR) is proposed in the paper. Firstly, in view of the self-adaptive weighted PSO featured by high precision and quick convergence, the method has made self-adaptive adjustment of systematic parameters based on PSO algorithm (with signal–noise ratio as fitness function). Secondly, GSTSR can further highlight the characteristic information otherwise covered by noise. Therefore, self-adaptive weighted PSO algorithm is combined with GSTSR to make characteristic extraction of rotor–stator rubbing faults. Finally, a comparative analysis with other methods and the analysis of faults in different states all indicate that the combination of self-adaptive weighted PSO algorithm and GSTSR can enhance rubbing fault characteristics and has effective identification of rotor–stator rubbing faults.

Keywords Rotor–stator rubbing · Fault identification · Stochastic resonance · Self-adaptive · Particle swarm optimization

H. Cong · M. Yu (✉) · Y. Gao · M. Fang
Shenyang Aerospace University, Shenyang, China
e-mail: yumingyue211@outlook.com

H. Cong
e-mail: chn91710@outlook.com

Y. Gao
e-mail: ggyyhh001@sina.com

M. Fang
e-mail: fmhmyn666@outlook.com

Introduction

Rotor–stator rubbing fault is one of the common faults in large-sized machinery, for example, aero-engine. Rubbing is harmful to the normal operation of equipment as a result of fierce body vibration and obvious rotate speed fluctuation of rotor. A serious rubbing fault will cause the divergency of amplitude of rotor and endanger the normal operation of equipment, resulting in a serious accident [1,2]. Scholars have paid great efforts to studying the effective identification of rotor–stator rubbing faults. Chen Xiangmin et al. took advantage of morphological component analysis [3] and Zhang Yongqiang et al. singular value decomposition algorithm [4] to distill impact elements of rotor rubbing fault signals and consequently implemented the effective diagnosis of rubbing faults. Yu et al. combined signal separation algorithm and graph signal processing in characteristic extraction and fault identification of rotor–stator rubbing fault [5]. Liu et al. separated fault signals with Fourier decomposition algorithm, constructed frequency-modulated and amplitude-modulated signals, and effectively solved the difficulty in extracting fault characteristic frequency of rotor [6].

To improve the SNR of signals and further highlight fault characteristics, a majority of signal analysis methods start with how to retrain and filter noises, such as wavelet threshold value denoising [7], coder denoising [8] and singular value denoising [9]. The study with this method of signal processing lies in retaining as much useful information as possible while suppressing noises. Stochastic resonance (SR), proposed by Italian scholars Benzi et al. [10–12] in 1981, differs with most of signal analysis methods, particular at improving SNR in using the noise to reinforce weak signals instead of eliminating. In 1998, Mitaim et al. [13] proposed self-adaptive

stochastic resonance which works by optimizing system parameters with various optimization algorithms and overcoming the defect of conventional stochastic resonance parameter in manual setting. At present, this algorithm has had wide application in fault diagnosis. For example, Quan Zhenya et al. self-adaptively obtained stochastic resonance parameter with cuckoo algorithm and combined with multipoint optimal minimum entropy deconvolution adjusted (MOMEDA). When bearings had weak faults, they successfully extracted the characteristic frequency of bearing fault [14]. Zhao et al. proposed self-adaptive stochastic resonance method underpinned by bat algorithm and verified the method based on fault signals of rolling bearings [15]. Yin proposed the stochastic resonance with synchronous parameter optimization, which could effectively detect weak fault signals from strong background noise and then made fault diagnosis [16]. Ren et al. proposed the combined method of self-adaptive stochastic resonance based on genetic algorithm and Fourier decomposition method. This approach effectively improves SNR and extracts the distinctive frequency of bearing fault signal [17]. Particle swarm optimization (PSO) algorithm was proposed by James Kennedy and Russell Eberhart on the basis of bird flock motion model [18]. Lai et al. proposed a method based on PSO bistable state stochastic resonance system and successfully extracted and diagnosed the fault characteristics of rolling bearings [19]. Zhang et al. proposed a self-adaptive variable step size stochastic resonance method based on PSO and effectively detected the rolling bearing fault signals in the context of strong noise [20].

It can be found that self-adaptive stochastic resonance has a vast application in the fault diagnosis of bearing, but less in the identification of rubbing faults. Considering that when a rubbing fault occurs, vibration signal is somewhat consistent with bearing fault signal (both will create impact components), the paper has combined adaptive weight PSO algorithm and general scale transformation stochastic resonance for identifying the rotor–stator rubbing faults. To validate the accuracy and effectiveness of method, a check analysis based on the proposed method has been given to the casing vibration signals from different running states. These states include: different running states (whether a rubbing fault or not), running extents (slight, medium and serious), running types (single-point and local rubbing) and casing thicknesses (4 mm and 7 mm).

Major Algorithm

Improved PSO Algorithm

To guarantee the performance of stochastic resonance in characteristic extraction, it is necessary to self-adaptively determine the system parameters a and b according to signals. PSO is a community cooperation intelligent search algorithm based on population information sharing. In PSO, feasible solution of optimization can be abstracted to a particle in m-dimension searching space, which only contains the information of location and speed [21]. It is featured by high precision and quick convergence. Based on that, the paper introduces PSO algorithm to self-adaptively determine the parameters a and b [22].

Inertia weight factor ω plays the most important part in adjusting global and partial optimization capacity of PSO algorithm. The larger the factor value is, the more powerful the global optimization capacity will be and the weaker the partial optimization capacity; otherwise, opposite. To reach a balance between global and partial optimization capacity of PSO algorithm, nonlinear dynamic inertia weight coefficient equation is used:

$$\omega = \begin{cases} \omega_{min} - \frac{(\omega_{max}-\omega_{min})*(l-l_{min})}{l_{avg}-l_{min}} & , l \le l_{avg} \\ \omega_{max} & , l > l_{avg} \end{cases} \quad \text{(Eq 1)}$$

where $\omega_{\max}$ and $\omega_{\min}$ separately represent the maximum and minimum value of ω; l, target function value of particle; and l_{avg} and $l_{\min}$, mean target value and minimum value of all particles. The name self-adaptive inertia weight refers to inertia weight varying with target function value, and the formula of speed and position update is shown as follows:

$$v_{ij}(t+1) = \omega v_{ij}(t) + c_1 r_1(t)\left[pbest_{ij}(t) - x_{ij}(t)\right] + c_2 r_2(t)\left[gbest_{ij}(t) - x_{ij}(t)\right] \quad \text{(Eq 2)}$$

$$x_{ij}(t+1) = x_{ij}(t) + v_{ij}(t+1) \quad \text{(Eq 3)}$$

In the formula, ω is the inertia weight factor; $v_{ij}(t+1)$, the speed of jth dimension of ith particle in tth iteration; $x_{ij}(t+1)$, position of jth dimension of ith particle in tth iteration (j=1, 2, …, D); *pbest*, optimal position of individual particle; *gbest*, optimal position of all particles; c_1 and c_2, learning factors; r_1 and r_2, uniform random number within the range [0,1].

Detailed PSO optimization process is shown in Fig. 1. The PSO fitness function is depicted as a 3D surface diagram in Fig. 1a. Figure 1b shows the original distribution diagram of particles. Figure 1c shows the diagram after optimization of fundamental particles (fixed inertia weight factor $\omega = 0.9$). Figure 1d shows the diagram after self-adaptive optimization of weight particles.

Through a comparison of Fig. 1c and d, it is easy to find that under the premise of self-adaptive weight, PSO algorithm has better capacity of exploration, development and optimization. Specifically, the procedure of improved PSO algorithm can refer to Ref. 23.

The fitness function is the most frequently used in PSO algorithm: signal–noise ratio (SNR). SNR is the ratio of signal and noise power and usually used to measure the

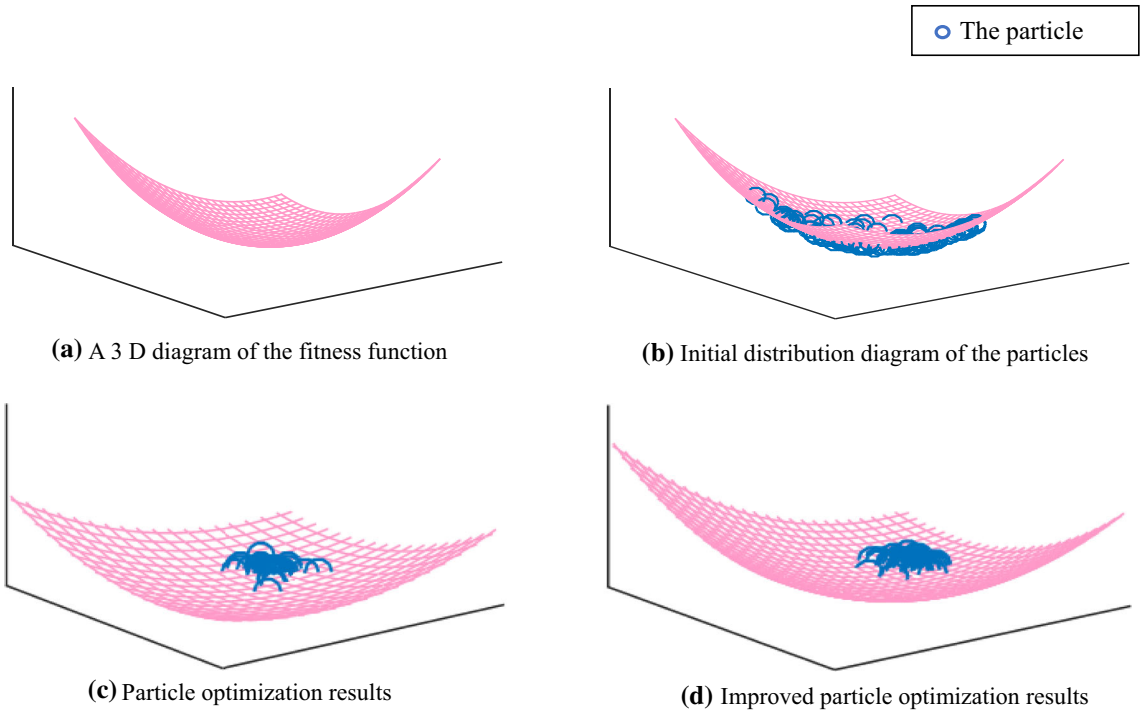

(a) A 3 D diagram of the fitness function

(b) Initial distribution diagram of the particles

(c) Particle optimization results

(d) Improved particle optimization results

Fig. 1 Particle search optimization comparison diagram of PSO and improved PSO

robustness of output properties and as the basis to evaluate the quality of signals. The SNR formula is shown as follows [24]:

$$\mathrm{SNR} = 10\lg\frac{P_0}{\left(\sum_{i=0}^{n} P_i - P_0\right)/n} \quad \text{(Eq 4)}$$

In the formula, n represents the number of time sequences, P_0 mean power of signal, and P_i the power of ith spot in time sequence. Generally speaking, the larger SNR the signal bears, the smaller noise the signal contains and the more characteristic information the signals contain; otherwise, opposite.

General Scale Transformation Stochastic Resonance

General scale transformation stochastic resonance can be matched to different high-frequency input signals with optimized barrier height to further improve output SNR and enhance weak signals. The second-order Lagrange equation of dimensionless underdamping bistable state system jointly driven by periodic signals and Gaussian white noise can be written as [25]:

$$\frac{d^2x}{dt^2} = ax - bx^3 - \gamma\frac{dx}{dt} + S(t) + N(t) \quad \text{(Eq 5)}$$

In Formula (5), $a > 0, b > 0$; γ is the damper factor; $S(t) = A\cos(2\pi ft)$ is the damper factor; $S(t) = A\cos(2\pi ft)$ periodic signals and A signal amplitude; f frequency of signal much larger than 1. $N(t) = \sqrt{2D}\xi(t)$ is Gaussian white noise in which D is the noise intensity and $\xi(t)$ is the standard Gaussian white noise with mean value and variance equal to 0 and 1. When m is a large enough constant, the GSTSR model of Formula (5) can be expressed as:

$$\frac{dz}{d\tau} = \frac{a}{m}z - \frac{b}{m}z^3 + \frac{A}{m}\cos\left(2\pi\frac{f}{m}\tau\right) + \sqrt{\frac{2D}{m}}\xi(\tau) \quad \text{(Eq 6)}$$

where m is the scale coefficient. After common variable scale, signal frequency is converted to the $1/m$ of original signal; amplitude and noise strength are reduced by $1/m$; through improved PSO algorithm, the optimal system parameter is m times of original. GSTSR is achieved based on classical fourth-order Runge–Kutta numerical discrete algorithm [26]. h represents the step size for calculation.

Proposed Method

To effectively detect rotor–stator rubbing fault, self-adaptive weight PSO algorithm is combined with GSTSR algorithm. Specific steps of the proposed method are shown in Fig. 2.

Details

(1) Input vibration signals into improved particle swarm optimization. With SNR as fitness function, output optimal system parameters a_1 and b_1.

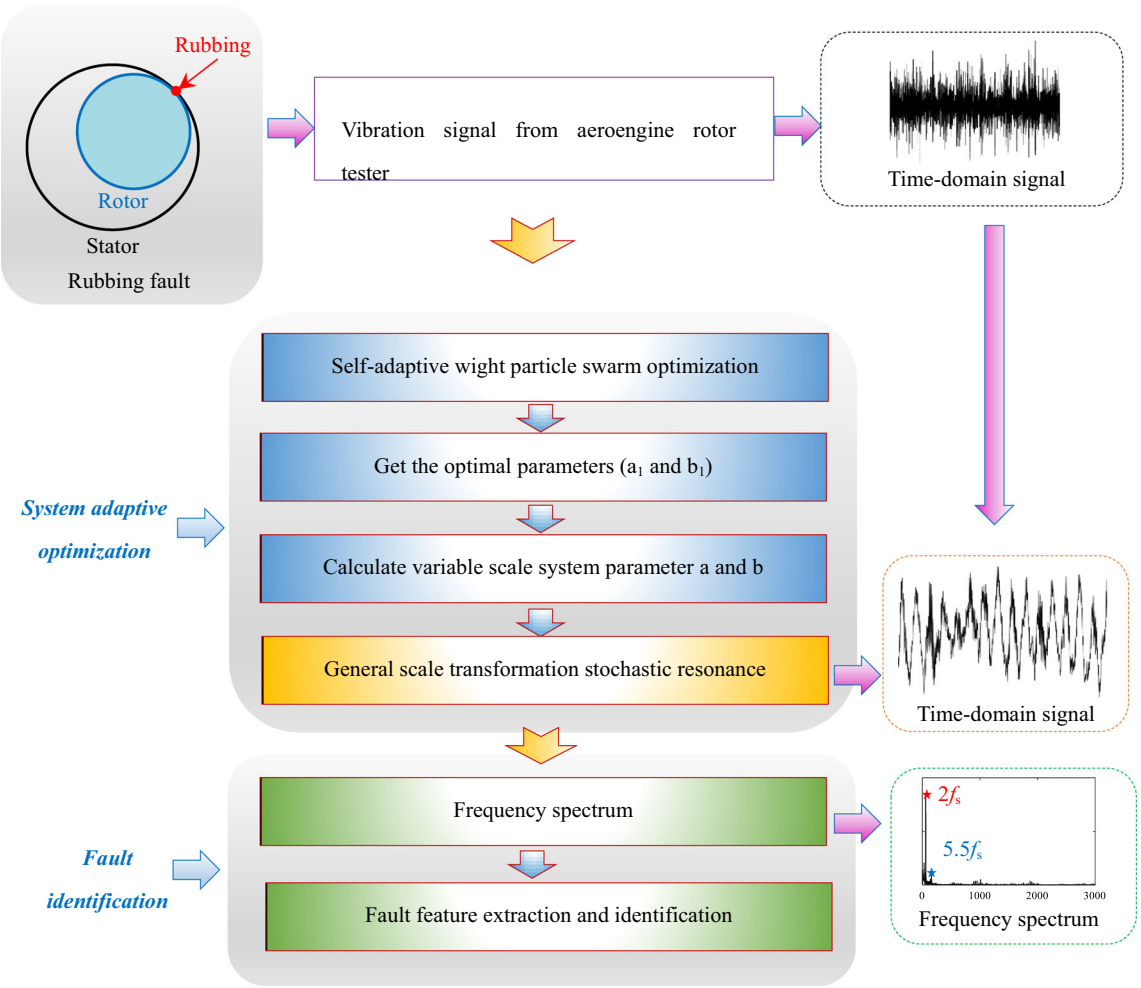

Fig. 2 Method block of the proposed method

(2) Calculate variable scale system parameters a and b according to scale coefficient.
(3) Based on obtained variable system parameters a and b and GSTSR algorithm, rubbing fault signals are subjected to self-adaptive stochastic resonance.
(4) According to the frequency spectrum of signals after self-adaptive stochastic resonance, extract features of the rubbing faults among the rotor and the stator and recognize fault types.

To verify the advantage of the proposed method, the proposed method of the literature [27] is combined with that of paper. The difference between two methods only lies in the determination of system parameters. The method of the literature [27] takes fixed ones (a = 1, b = 1, step size h = 0.2) for different fault signals, while the proposed method of paper introduces self-adaptive particle swarm algorithm to determine system parameters according to different fault signals.

Experiments of Rotor–Stator Rubbing Fault

The experimental data have been collected from rotor tester of aero-engine shown in Fig. 3a. The details of experiment are included in Ref. 28. The tester is able to simulate the typical faults which may happen in aero-motor, for example, point rubbing and partial rubbing. Figure 3b, c shows the installation positions of acceleration sensors and rubbing positions in single-point rubbing experiment (casing thickness 4 mm). The channel configuration of each sensor is shown in Table 1. Figure 3d shows turbine casings of different thicknesses. The installation position of the acceleration sensor is presented in Fig. 3e and rubbing position in single-spot rubbing experiment when casing thickness is 7 mm. (The installation position of sensor on thick-wall casing is the same as that on thin-wall casing, but rubbing position is on upper right, lower right, lower left and upper left of casing.) Figure 3f shows the partial rubbing experiment in which experiment devices are adjusted to achieve the goal. Limited by the length of the

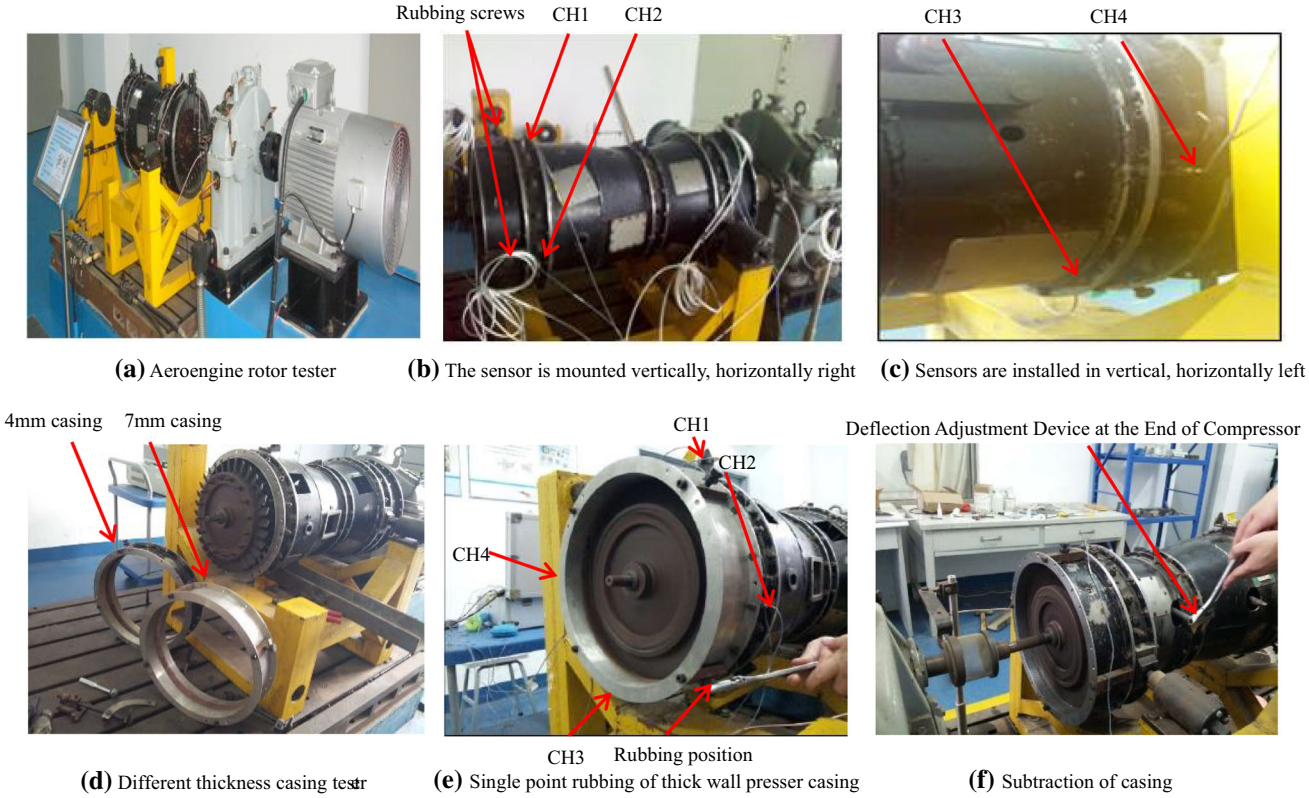

(a) Aeroengine rotor tester **(b)** The sensor is mounted vertically, horizontally right **(c)** Sensors are installed in vertical, horizontally left

(d) Different thickness casing tester **(e)** Single point rubbing of thick wall presser casing **(f)** Subtraction of casing

Fig. 3 Rotor rubbing fault test

Table 1 Channel configuration

Channel	Sensor installation position
CH1	Turbine casing vertical on
CH2	Turbine casing horizontal right
CH3	Turbine casing vertical under
CH4	Turbine casing horizontal left

paper, we only choose the rubbing experiment on the ends of compressor. (Experiment results from turbine end are similar to that of compressor.) In the experiment, acceleration sensors are still installed on turbine. Details of rubbing experiment, such as running state, rubbing type, rubbing position, installation position of sensor (facing toward turbine casing as standard), rubbing extent, casing thickness and experimental rotate speed, are shown in Table 2. Acceleration sensor used in simulation experiment is model 4508, and the sampling frequency is 10000Hz.

Case Analysis

For verifying the accuracy and superiority of the proposed new method, a comparative analysis is given to the presented method of Ref. 27 (the parameters of stochastic resonance system serve as empirical value) and the result of comparison is validated. (Fitness functions of two methods are both SNR.)

Firstly, randomly taking the data of rubbing the horizontal left of casing as an example (randomly opt for the vibration acceleration signals (CH3) collected by sensor below the casing), analysis and comparative validation have been carried out. The corresponding rotate speed is 1726.33r/min, and the rotate frequency (f_s) is 28.77Hz. The rubbing extent is slight, and the casing thickness is 4mm.

Method of Ref. 27

Firstly, based on the presented method of Ref. 27, extract the features of rubbing faults. The result is presented in Fig. 4. The difference between Ref. 27 and the proposed method only lies in the determination of system parameters. The method of the literature [28] takes fixed ones (a = 1, b = 1, step size h = 0.2) for different fault signals. Figure 4a1 proves the time domain of vibration acceleration signals, and 4b1 shows the frequency spectrum of a1. According to Ref. 27, the empirical value and step size of a and b can be obtained h (a = 1, b = 1, h = 0.2) and vibration signals are subjected to stochastic resonance. Figure 4a2 shows the time domain of output signals after stochastic resonance and b2 is the frequency spectrum of a2.

Table 2 Statistics of experimental data

Cases	Running status	Rubbing type	Rubbing position	Sensor selected	Degree of rubbing	Thickness of casing (mm)	Rotation speed (r/min)
Case 1	Fault	Single-point	Horizontal left	Under	Minor	4	1726.33
Case 2	Normal	…	…	Left	…	4	1745.31
Case 3	Fault	Single-point	Vertical on	Under	Serious	4	1739.26
Case 4	Fault	Partial	Partial left	Under	Medium	4	1236.52
Case 5	Fault	Single-point	Left upper	On	Medium	7	1230.18

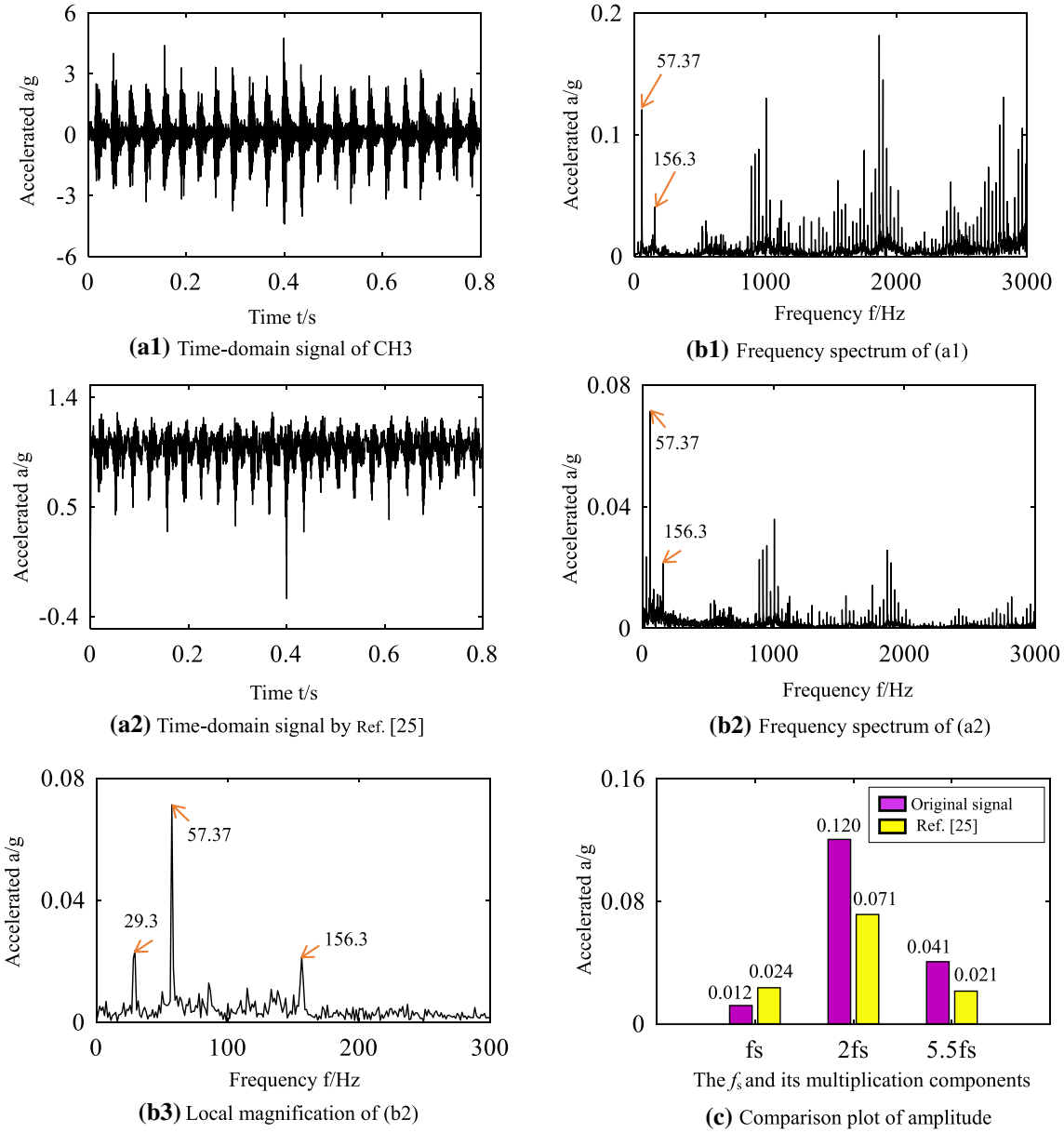

(a1) Time-domain signal of CH3

(b1) Frequency spectrum of (a1)

(a2) Time-domain signal by Ref. [25]

(b2) Frequency spectrum of (a2)

(b3) Local magnification of (b2)

(c) Comparison plot of amplitude

Fig. 4 Rotor–stator rubbing feature extraction based on Ref. 27

Figure 4b3 shows the partial enlarged drawing of Fig. 4b2. Figure 4c shows the comparison of b1 and b2 in rotation frequency and multiplications.

Firstly, it can be found from the analysis of Fig. 4b1 that there is evident 2x of rotate frequency ($2f_s$=57.37Hz) and 5.5x ($5.5f_s$=156.3Hz) in the frequency spectrum of original

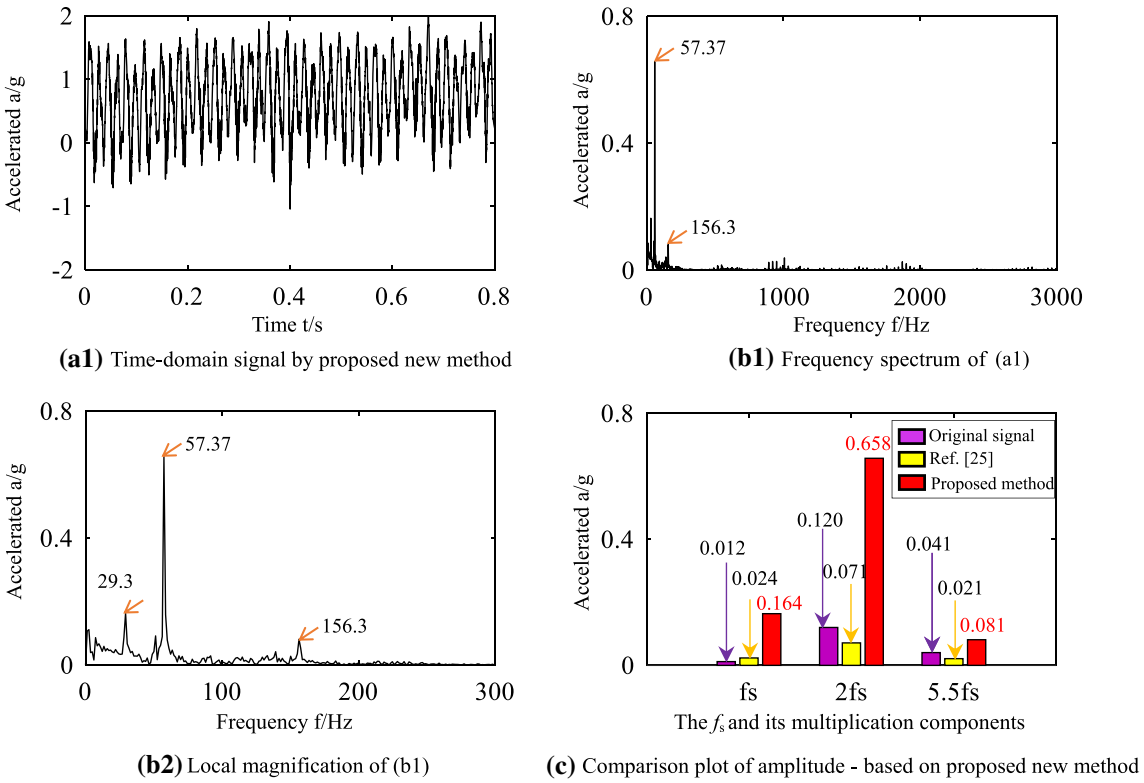

(a1) Time-domain signal by proposed new method

(b1) Frequency spectrum of (a1)

(b2) Local magnification of (b1)

(c) Comparison plot of amplitude - based on proposed new method

Fig. 5 Rotor–stator rubbing feature extraction based on the proposed new method

signal. But noise components are large, and high-frequency signals are highlighted in frequency spectrum.

Secondly, it can be found from the result (Fig. 4b2 and b3) of the proposed method of the literature [27] that there is typical rotate frequency (f_s = 29.3Hz) and its 2x ($2f_s$ = 57.37Hz) and 5.5x ($5.5f_s$=156.3Hz) in the frequency spectrum of signals. Meanwhile, high-frequency components are decreased and characteristics of low-frequency components are comparatively highlighted, further highlighting the characteristic frequency of rubbing faults.

Finally, further analysis can reveal the following limits of the literature [27]: Compared with the frequency spectrum of original signals, amplitude of rotation frequency multiples decreases (Fig. 4c). (The amplitude of rotation frequency f_s increases from 0.012 to 0.024.) Meanwhile, the frequency components irrelevant to the type of faults are still in large number. They are all disadvantageous to the identification of rubbing faults.

Proposed New Method

To further highlight features of rubbing faults and improve the performance of identification, next, the proposed new method (shown in Fig. 2) will be used for extracting the features of rubbing faults. For a comparison and validation, the experimental data chosen are entirely the same with Section "Method of Ref. 27". The time domain and frequency spectrum of vibration acceleration signals are still as shown in Fig. 4a1 and b1. After the improvement in particle swarm optimization of signals, optimal parameter $a_1 = 1.5516, b_1 = 1.0985$ can be obtained. Given m=100, optimal parameter of system $a = 0.015516, b = 0.010985$ can be acquired with step size h=0.2. (h is entirely the same with Section"Method of Ref. 27") Based on the optimal a and b, signals are treated by general scale transformation SR and the result is as shown in Fig. 5. Figure 5a2 shows the time domain of output signals after stochastic resonance, and 5b2 shows the frequency spectrum of 5a2. Figure 5b2 shows the partial enlarged drawing of Fig. 5b1. Figure 5c shows the comparison of amplitudes of rotation frequency and the frequency multiplication of each method. For a comparison, Table 3 lists the SNR of original signal, output signal of Ref. 27 and the one obtained based on the proposed new method.

Table 3 The SNR of original signal and output signal by Ref. 27 and proposed method (Unit: dB)

	Original signal	Ref. 27	Proposed method
SNR	−20.0375	−22.9603	4.4487

Through the analysis of Fig. 5b1, b2 and c and a comparison between 5b1 and 4b2, 5b2 and 4b3, it can be found

that the frequency spectrum of signals obtained based on the proposed new method of paper has the following characteristics:

There is typical and highlighted 1x (f_s = 29.3Hz), 2x ($2f_s$ = 57.37Hz) and 5.5x ($5.5f_s$ = 156.3Hz) of rotation frequency, which further highlights the characteristic frequency of rubbing faults. Compared with original signals and the scheme proposed by the literature [27], the amplitude of rubbing characteristic frequency obtained by the proposed method (rotation frequency and its multiples) sees significant improvement. For example, the amplitude of 2x ($2f_s$ = 57.3Hz) of rotation frequency increases from 0.07 to 0.658, almost 10 times higher. Meanwhile, high-frequency components and the ones irrelevant to fault characteristics are largely reduced and characteristic components of fault further highlighted.

It can be known from Table 3 that the proposed new method can obtain the SNR of output signal obviously higher than the one of original vibration signals and the proposed method of Ref. 27.

Namely, no matter from the SNR of output signals or the strength (amplitude) of characteristic frequency of fault in spectrum, the proposed new method of paper is obviously superior to Ref. 27 in the performance of characteristic extraction of rubbing fault.

An Analysis of Effectiveness of Method in Each State

To verify the effectiveness and veracity of the proposed new method in extracting rubbing fault characteristics of rotor and stator in different situations, we will implement characteristic extraction and fault identification based on the proposed new method of paper with the casing vibration acceleration signals collected from different running states, rubbing extents, rubbing types and casing thicknesses.

Normal Running

Firstly, analyze the accuracy of rubbing fault identification. Randomly choose the acceleration signal (CH4) detected by the sensor left as an example in normal running state. The rotate speed is 1745.31r/min, the rotation frequency (f_s) is 29.08 Hz, and the casing thickness is 4mm. Figure 6a1 shows the time domain wave of vibration signal, and 6(b1) shows the frequency spectrum of 6(a1). After fault signals are treated by improved PSO, we can obtain optimal parameter $a_1 = 1.8317, b_1 = 2.7641$. Given m=100, $a = 0.018317, b = 0.027641$ and step size is consistent with Section "Method of Ref. 27" (h = 0.2). Signals are treated by general scale transformation SR based on optimal a and b values. Figure 6a2 shows the time domain of output signals after stochastic resonance, and 6b2 shows the frequency spectrum of 6a2. Table 4 shows original vibration signals and the SNR of output signals based on the proposed method.

Analyzing Fig. 6b1 and b2 and comparing it with Fig. 5b1, we can find that the proposed new method has the following features:

When the tester runs normally, the high-frequency components are largely reduced in the frequency spectrum of signal (Fig. 6b2). Meanwhile, there is only 1x of rotation frequency (f_s=29.3Hz). Thus, it can be judged that there is no rubbing fault in the equipment. This can recognize the running state of equipment. It can be known from Table 4 that based on the proposed method, the SNR of signal increases from −16.6301 to 6.0623 and output SNR has significant improvement.

Namely, the proposed new method can largely reduce noise component, improve SNR and have effective monitoring on running state of equipment (with a rubbing or not).

Different Rubbing Extents

Next, we will analyze the effectiveness of the proposed method according to different rubbing extents. Randomly take the vibration acceleration signal (CH3) detected by the sensor below turbine casing as an example when rubbing casing is vertically upward. The rotate speed is 1739.26r/min, the rotation frequency (f_s) is 28.98Hz, the rubbing extent is serious, and the casing thickness is 4mm. Figure 7a1 remains the time domain of vibration acceleration signals, and 7(b1) shows the frequency spectrum of (a1). After fault signals are treated by improved PSO, we can obtain optimal parameter $a_1 = 1.5648, b_1 = 1.3214$. Given m=100, $a = 0.015648, b = 0.013214$ and step size is consistent with Section "Method of Ref. 27" (h = 0.2). Signals are treated by general scale transformation SR based on optimal a and b values. Figure 7a2 shows the time domain of output signals after stochastic resonance, and 7b2 shows the frequency spectrum of 7a2. Figure 7c shows the comparison of 7b1 and b2 in rotation frequency and multiplications. Table 5 shows the SNR of original vibration signals and the ones obtained by the proposed new method when rubbing extents are different.

With the analysis of Fig. 7b1, b2 and c, the frequency spectrum of signals based on the proposed new method in different rubbing extents has the following characteristics:

In the frequency spectrum, there is obvious 2x and 5.5x of rotation frequency ($2f_s$=58.59Hz, $5.5f_s$=157.5Hz). It can be judged that there is a rubbing fault in the equipment. Meanwhile, compared with the frequency spectrum of original signal, noise components are largely reduced and amplitude of rubbing characteristic frequency has

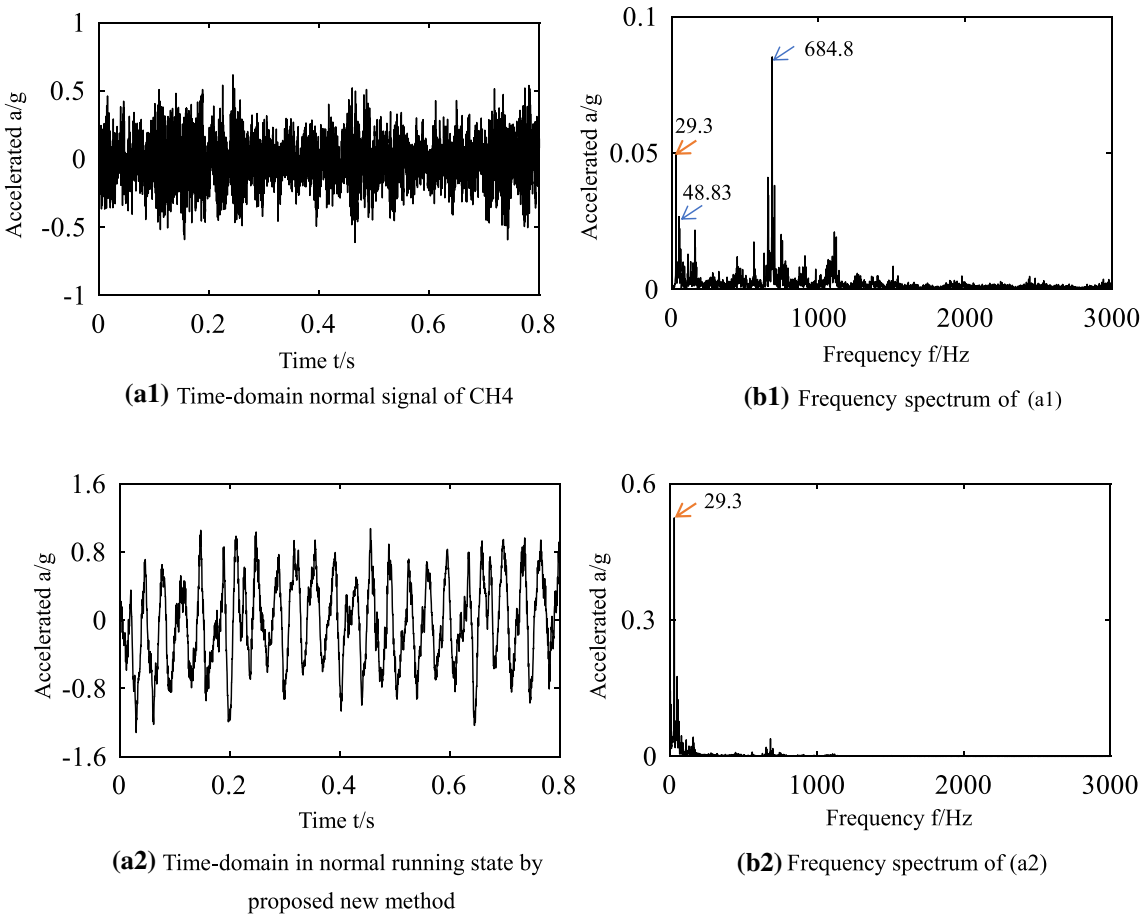

(a1) Time-domain normal signal of CH4

(b1) Frequency spectrum of (a1)

(a2) Time-domain in normal running state by proposed new method

(b2) Frequency spectrum of (a2)

Fig. 6 Rotor–stator rubbing feature extraction in different running states—proposed method

Table 4 The SNR in different running states (Unit: dB)

	Original signal	Proposed method
SNR	−16.6301	6.0623

significant improvement, highlighting the characteristics of rubbing fault.

It can be known from Table 5 that based on the proposed method, the SNR of signal increases from -23.6848 from 8.5960 and the SNR of output signal has a great improvement.

Namely, the proposed new method of paper can still greatly reduce noise components, improve SNR and correctly and effectively identify rubbing faults when rubbing extents are different.

Different Rubbing Fault Type

The next is the effectiveness analysis of the proposed method for different rubbing faults. Randomly choose the vibration acceleration signal (CH3) detected by the sensor below as an example when the end of compressor is inclined to left. The corresponding rotate speed is 1236.52r/min, the rotation frequency (f_s) is 20.61Hz, the rubbing extent is moderate, and the casing thickness is 4mm. Figure 8a1 shows the time domain of vibration acceleration signals, and 8(b1) shows the frequency spectrum of (a1). After fault signals are treated by improved PSO, we can obtain optimal parameter $a_1 = 1.1085, b_1 = 0.8587$. Given m=100, $a = 0.011085, b = 0.008587$ and step size is consistent with Section "Method of Ref. 27" (h = 0.2). Signals are treated by general scale transformation SR based on optimal a and b values. Figure 8a2 shows the time domain of output signals after stochastic resonance, and 8b2 shows the frequency spectrum of 8a2. Figure 8c shows the comparison of 8b1 and b2 in rotation frequency and multiplications. Table 6 shows the SNR of original vibration signal and the ones obtained by the proposed new method when rubbing fault type is different.

With the analysis of Fig. 8b1, b2 and c, when partial rubbing fault happens in the system, namely, in the different rubbing types, the proposed new method of paper has the following characteristics:

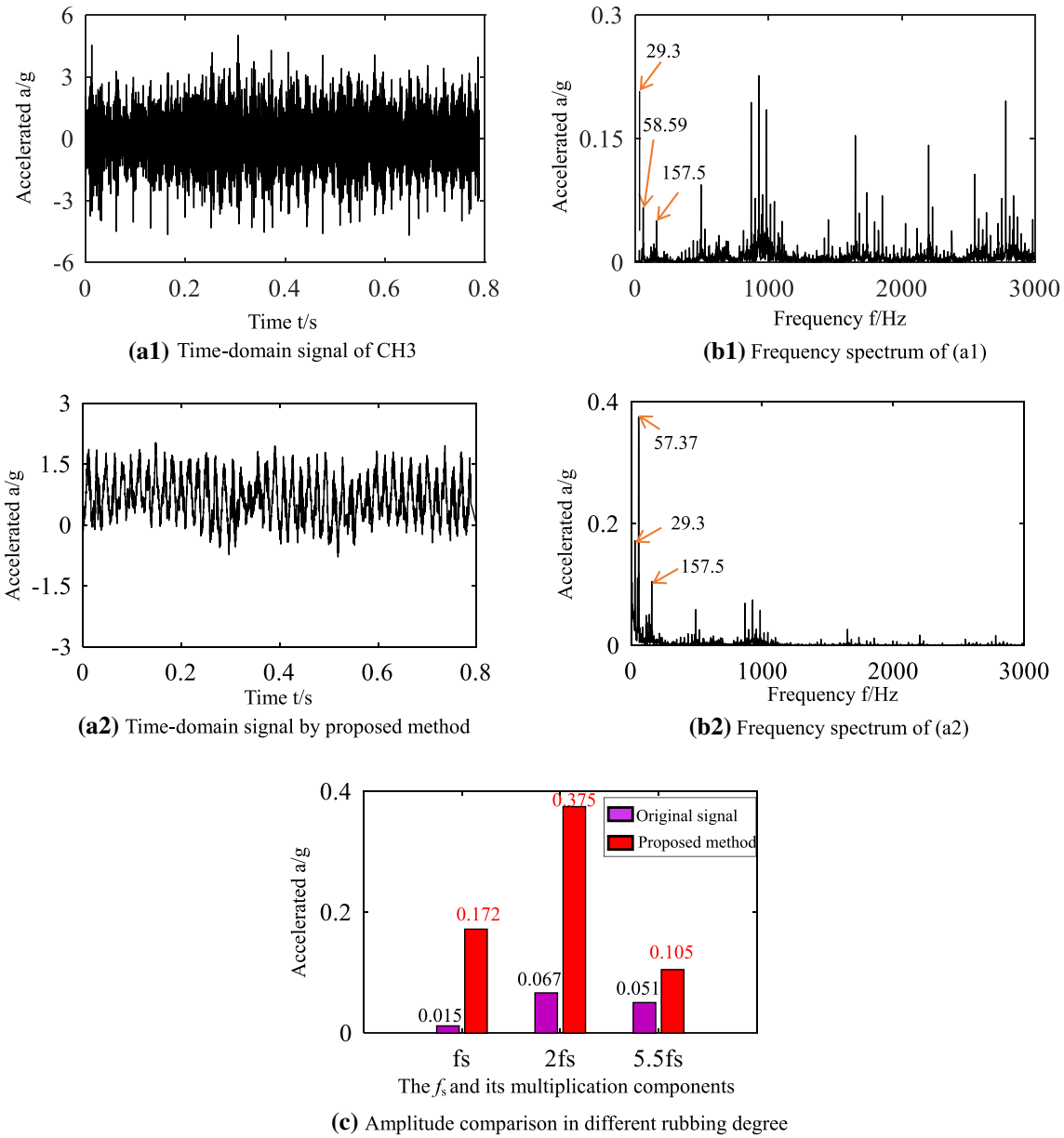

(a1) Time-domain signal of CH3

(b1) Frequency spectrum of (a1)

(a2) Time-domain signal by proposed method

(b2) Frequency spectrum of (a2)

(c) Amplitude comparison in different rubbing degree

Fig. 7 Rotor–stator rubbing feature extraction in different rubbing degrees—proposed method

Table 5 The SNR in different rubbing degrees (Unit: dB)

	Original signal	Proposed method
SNR	−23.6848	8.5960

Frequency components are more complex than single-point rubbing, but there is obvious 2x ($2f_s$ = 40.28Hz) of rotation frequency. Compared with frequency spectrum of original signal, noise components are largely reduced. Meanwhile, characteristics of rubbing fault are more obvious. (Amplitude of 2x and 5.5x frequency components has been improved.)

It can be learnt from Table 6 that the SNR of signal increases from -26.0935 to -0.6531 and output signal SNR is clearly improved.

That means the proposed new method can still greatly reduce noise components and improve SNR when rubbing type is local partial rubbing. Meanwhile, though the frequency components in frequency spectrum are more complex than single-spot rubbing, it can still precisely and effectively identify the type of rubbing fault.

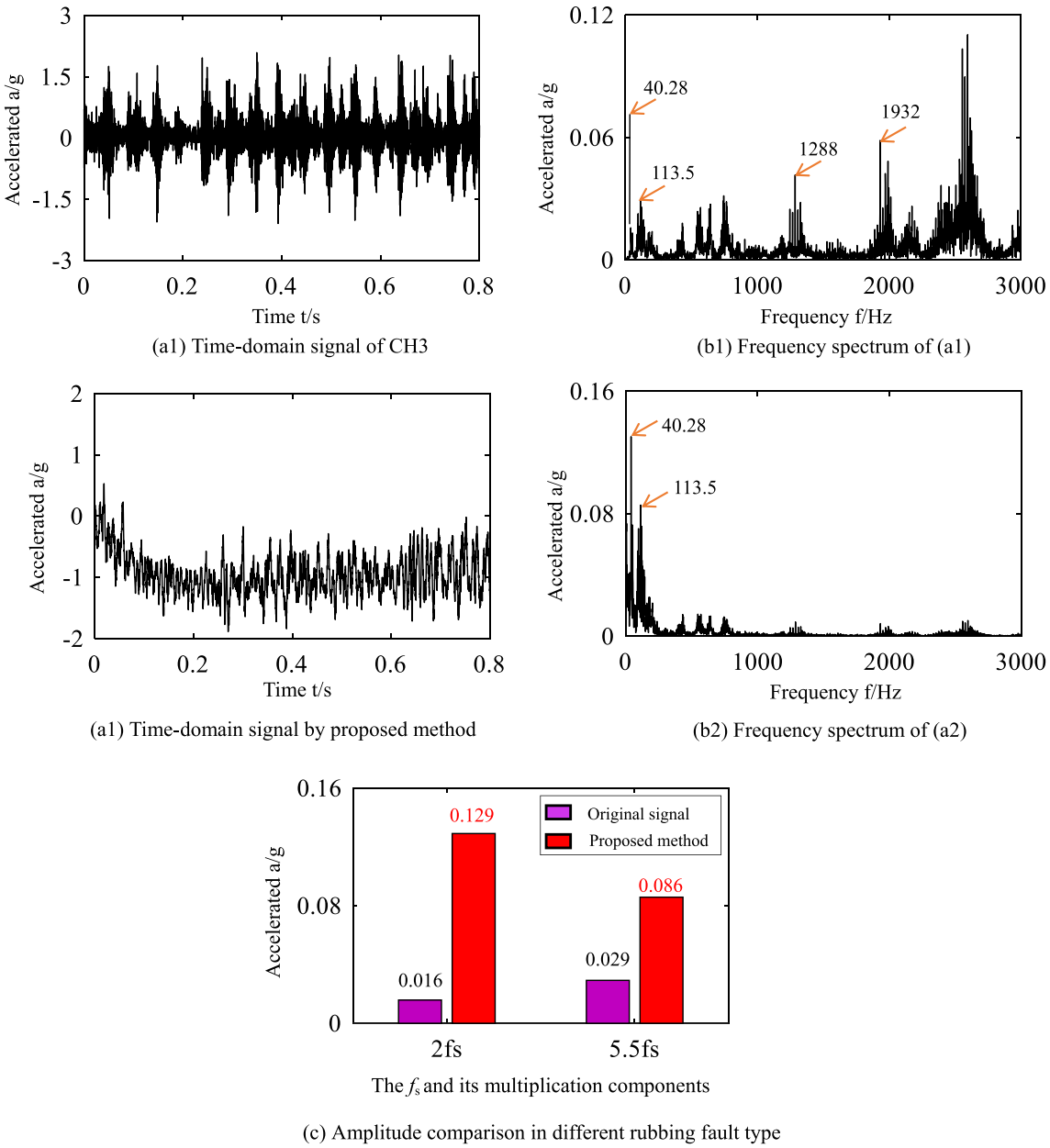

Fig. 8 Rotor–stator rubbing feature extraction in different rubbing fault types—proposed method

Table 6 The SNR in different rubbing fault types (Unit: dB)

	Original signal	Proposed method
SNR	−26.0935	−0.6531

Different Casing Thicknesses and Rubbing Positions

Finally, we will carry out the effectiveness analysis for different casing thicknesses. When rubbing against the upper left of casing, randomly take the vibration acceleration signal (CH1) detected by the sensor upper as an example. The rotate speed is 1230.18r/min, the rotation frequency (f_s) is 20.50Hz, the rubbing extent is moderate, and the casing thickness is 7mm. Figure 9a1 remains the time domain of vibration acceleration signals, and 9(b1) shows the frequency spectrum of (a1). After fault signals are treated by self-adaptive weight PSO, we can obtain optimal parameter $a_1 = 1.8163, b_1 = 1.2457$. Given m=100, $a = 0.018163, b = 0.012457$ and step size is consistent with Section "Method of Ref. 27" (h = 0.2). Signals are treated by general scale transformation SR based on optimal a and b values. Figure 9a2 shows the time domain of output signals after stochastic resonance, and 9(b2) shows the frequency spectrum of 9a2. Figure 9c shows the

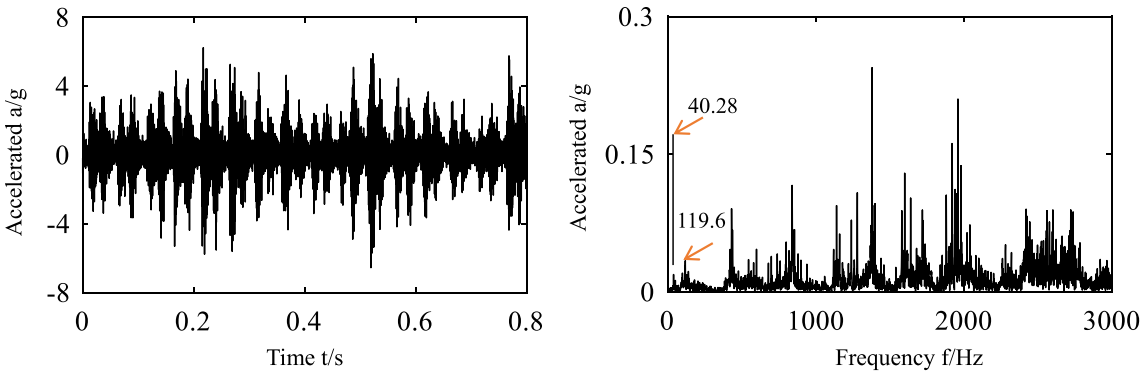

(a1) Time-domain signal of CH

(b1) Frequency spectrum of (a1)

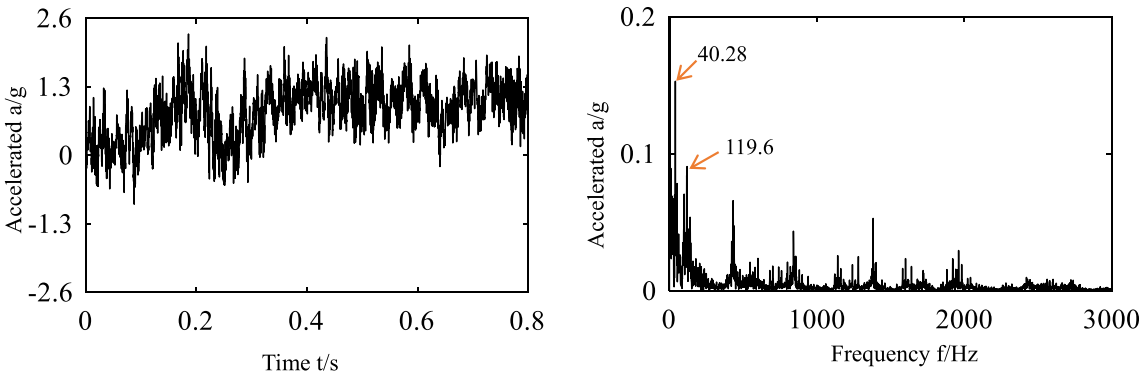

(a2) Time-domain signal by proposed method

(b2) Frequency spectrum of (a2)

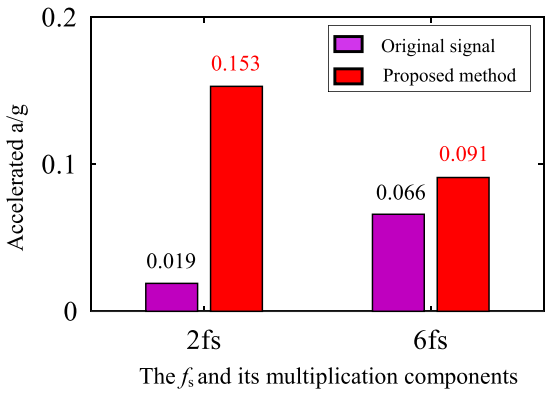

(c) Amplitude comparison in different casing thickness and rubbing position

Fig. 9 Rotor–stator rubbing feature extraction in different casing thicknesses and rubbing positions—proposed method

comparison of 9b1 and b2 in rotation frequency and multiplications. Table 7 shows the SNRs of original vibration signals and the ones obtained by the proposed new method when the casing thickness and rubbing position are different.

It can be found from the analysis of Fig. 9b1, b2 and 9c that when casing thickness and rubbing position are different, the proposed new method of paper has the following features:

There is obvious 2x and 6x frequency component of rotation frequency ($2f_s$=40.28Hz, $6f_s$=119.6Hz). Compared with the frequency spectrum of original signals, noise components are sharply reduced and characteristic frequency of fault is further highlighted. (Amplitude of frequency component has obvious improvement.)

Table 7 The SNR in different casing thicknesses and rubbing positions (Unit: dB)

	Original signal	Proposed method
SNR	−18.2128	−1.6018

Compared with thin-walled casing, there are more frequency components in frequency spectrum.

It is known from Table 7 that when casing thickness is 7mm, the SNR of signal based on the proposed new method increases from −18.2128 to −1.6018 and output SNR has significant improvement.

Namely, the proposed new method of paper can still greatly reduce noise components and improve SNR when casing thickness varies. Meanwhile, though the frequency components are more complicated than that of thin-wall casing (4mm), the proposed new method can still precisely and effectively recognize a rubbing fault.

Conclusion

To effectively and precisely identify a rotor–stator rubbing fault, the paper has introduced the combined method of adaptive weight PSO and GSTSR. An analysis has been given to the fault data in various states, and the following conclusions can be drawn:

①Improved method of PSO and common variable scale stochastic resonance can effectively identify the running state of equipment (if a rubbing fault or not).

②After self-adaptively determining system parameter with PSO algorithm, high-frequency components are largely reduced and output SNR is significantly improved in the frequency spectrum of signal. Meanwhile, the frequency components irrelevant to rubbing fault characteristics in the spectrum are largely reduced, further highlighting the characteristic frequency of rubbing fault. (Amplitude of characteristic frequency of rubbing fault is largely increased.) That is the combination of PSO and stochastic resonance can self-adaptively determine system parameter.

③The proposed new method is insensitive to rubbing extent (slight, moderate and serious), rubbing type (single-spot rubbing and partial rubbing), casing thickness (4mm, 7mm) and rubbing position. In various situations, the proposed method can equally extract obvious characteristic components of rubbing faults and implement effective identification.

Acknowledgment This work was supported by the National Natural Science Foundation of China [Grant number: 51605309], Natural Science Foundation of Liaoning Province [Grant number: 2019-ZD-0219] and Aeronautical Science Foundation of China [Grant number: 201933054002].

Declarations

Conflict of interest The authors declare no conflict of interest in preparing this article.

References

1. Y. L. Jin, Z. W. Liu, Y. S. Chen. Simulation of blade casing rubbing for a dual-rotor system of an aero-engine. Acta Aeronautica et Astronautica Sinica: 2021, 42 (**in Chinese**)
2. W.M. Wang, Z.W. Chen, X.L. Zhang, K. Chen, Fault diagnosis method of rotor rubbing impact based on blade tip timing [J/OL]. Acta Aeronaut. et Astronaut. Sinica. **9**(23), 1–11 (2021)
3. X.M. Chen, D.J. Yu, X. Li, R. Li, Early rub-impact diagnosis of rotors using morphological component analysis. J. Vibr. Eng. **27**(03), 466–472 (2014)
4. Y.Q. Zhang, L. Yi, The extraction of the fault features from aero-engine rotor contact-rubbing based on singular value decomposition. Chin. J. Appl. Mech. **36**(02), 260–266 (2019)
5. M.Y. Yu, A novel intrinsic time–scale decomposition–graph signal processing–based characteristic extraction method for rotor–stator rubbing of aeroengine. J. Vibr. Control. (2021). https://doi.org/10.1177/1077546320985968
6. Y. Liu, X.B. Liu, S. Liang, Aeroengine rotor fault diagnosis based on Fourier decomposition method. China Mech. Eng. **30**(18), 2156–2163 (2019)
7. F.S. Xu, X.W. Sun, Z.X. Dong, H.Y. Wang, H.R. Yang, Research on noise reduction method based on novel wavelet threshold function. Mech. Eng. Autom. **05**, 23–24 (2021)
8. J. Zhou, M. Yang, Y. Yin, Research on acoustic emission signal denoising based on autoencoder. J. Phys. Conf. Series. **2031**(1), 012001 (2021)
9. G.Y. Pan, S.M. Li, H.R. Du, Y.Q. Zhu, Feature extracting method for gearbox tooth breakage under impact based on the S-transform time-frequency spectrum combined with the denoising by SVD. J. Vibr. Shock. **38**(18), 256–263 (2019)
10. R. Benzi, A. Sutera, A. Vulpiani, The mechanism of stochastic resonance. J. Phys. A Math. Gen. **14**(11), 453–457 (1981)
11. T. Zheng, S.P. Li, S.J. Cheng, X.M. Wu, The research of related parameters in twice sampling stochastic resonance used in week signal detection. Acta Metrol. Sinica. **36**(03), 313–317 (2015)
12. W.J. Cai, F.Z. Wang, H.C. Zhang, H.H. Lu, Weak speech enhancement based on stochastic resonance and spectral subtraction. Comput. Eng. Design. **39**(02), 499–502 (2018)
13. S. Mitaim, B. Kosko, Adaptive stochastic resonance[J]. Proc. IEEE. **86**(11), 2152–2183 (1998)
14. Z.Y. Quan, X.L. Zhang, Rolling bearing weak fault feature extraction based on multipoint optimal minimum entroy deconvolution adjusted and adaptive stochastic resonance with cuckoo search. J. Mech. Strength. **43**(04), 771–778 (2021)
15. P.Z. Zhao, J. Liu, Bearing fault diagnosis of high-speed EMUs based on stochastic resonance and bat algorithm. China Meas. Test. **47**(03), 16–23 (2021)
16. J.T. Yin, J. Tang, L. Liu, X.B. Liu, Z.H. Peng, H. Li, Application of parameter synchronous optimization stochastic resonance in early weak fault diagnosis of traction drive system. J. Vibr. Shock. **40**(17), 234–240 (2021)
17. Y. Ren et al., Research on fault feature extraction of Hydropower units based on adaptive stochastic resonance and Fourier decomposition method. Shock Vibr. **2021**, 1–12 (2021)
18. J. Kennedy, R. Eberhart, Particle swarm optimization. Proc. IEEE Int. Conf. Neural Netw. **4**, 1942–1948 (1995)
19. Z.H. Lai et al., Rolling bearing fault diagnosis based on adaptive multiparameter-adjusting bistable stochastic resonance. Shock Vibr. **2020**, 1–15 (2020)
20. Z.H. Zhang, D. Wang, T.Y. Wang, J.Z. Lin, Y.X. Jiang, Self-adaptive step-changed stochastic resonance using particle swarm optimization. J. Vibr. Shock. **32**(19), 125–130 (2013)
21. Z.X. Wang, L. Guo, Research on weak signal detection method based on adaptive stochastic resonance. Comput. Meas. Control.

26(01), 42–46 (2018). https://doi.org/10.16526/j.cnki.11-4762/tp.2018.01.011
22. J. Zhang, M. Zhong, J.Q. Zhang, L.G. Yao, J.D. Zheng, An integrating methodology of teager energy operator and stochastic resonance for incipient fault diagnosis of planetary gearboxes. J. Vibr. Eng. **32**(06), 1084–1093 (2019). https://doi.org/10.16385/j.cnki.issn.1004-4523.2019.06.018
23. J.H. Han, Z.R. Li, Z.C. Wei, Adaptive particle swarm optimization algorithm and simulation. J. Syst. Simul. **10**, 2969–2971 (2006)
24. V. Gandhimathi, K. Murali, S. Rajasekar, Stochastic resonance in overdamped two coupled anharmonic oscillators. Phys. A Stat. Mech. Appl. **347**(347), 99–116 (2005)
25. D.W. Huang, J.H. Yang, C.Q. Tang, J.L. Zhang, H.G. Liu, General scale transformation stochastic resonance of the second-order system and bearing fault diagnosis. J. Vibr. Meas. Diagn. **38**(06), 1260–1266 (2018)
26. Q. Liang, S.M. Wang, Study on stochastic resonance theory for weak signal detection. Meas. Control Technol. **09**, 76–78 (2007)
27. Y. Lv, Y. Zeng, F.B. Zheng, B. Hou, Application of stochastic resonance to early rub-impact faults signal in rolling bearing-rotor system. Mar. Electr. Electron. Eng. **35**(05), 10–13 (2015)
28. G. Chen, G.Q. Feng, G.Y. Jiang, C.G. Li, D.Y. Wang, Feature analysis and verification of casing vibration acceleration for aeroengine blade-casing rubbing fault. Aeroengine. **40**(01), 10–16 (2014)